Supporting Information

Biodegradable Core-shell Dual-Metal-Organic-Frameworks Nanotheranostic Agent for Multiple Imaging Guided Combination Cancer Therapy

Dongdong Wang,[1*] Jiajia Zhou,[2*] Ruohong Shi,[1] Huihui Wu,[2] Ruhui Chen,[1] Beichen Duan,[1] Guoliang Xia,[1] Pengping Xu,[1] Hui Wang,[3] Shu Zhou,[2] Chengming Wang,[1] Haibao Wang,[4✉] Zhen Guo,[2✉] and Qianwang Chen[1,3✉]

1.Hefei National Laboratory for Physical Sciences at Microscale, Department of Materials Science & Engineering & Collaborative Innovation Center of Suzhou Nano Science and Technology, University of Science and Technology of China, Hefei, 230026, China.
2.Anhui Key Laboratory for Cellular Dynamics and Chemical Biology, School of Life Sciences, University of Science and Technology of China, Hefei, 230027, China.
3.High Magnetic Field Laboratory, Hefei Institutes of Physical Science, Chinese Academy of Sciences, Hefei, 230031, China.
4.Radiology Department of the First Affiliated Hospital of Anhui Medical University, Hefei, 230022, China.
[*]Equal contribution to this study.
[✉]Corresponding Authors: Haibao Wang, E-mail: wanghaibao916@163.com; Zhen Guo, E-mail: zhenguo@ustc.edu.cn; Qianwang Chen, E-mail: cqw@ustc.edu.cn

1. Experimental Section

1.1. Materials:

Zinc nitrate ($Zn(NO_3)_2 \cdot 6H_2O$, 99.0%), 2-methylimidazole (2-MeIM, 99.0%), (Poly(vinylpyrrolidone), PVP, K-30), concentrated hydrochloric acid (HCl, 36.0-38.0%) and $K_3[Fe(CN)_6]$ were purchased from Sinopharm (Shanghai) Chemical Reagent Co., Ltd., China. Poly(sodium-4-styrenesulfonate) (PSS, Aldrich, average M_W: 2200). Doxorubicin (DOX) was purchased from Shanghai Sangon Biotech Company (Shanghai City, China). Aqueous solutions were prepared with deionized water (18.2 MΩ·cm) produced from a Milli-Q water purification system. All other chemicals used in this work were of analytical grade, obtained from commercial suppliers, and used without further purification unless otherwise noted.

1.2. Preparation of PB@ZIF-8 CSD-MOFs:

The preparation of PB was operated according to our previous report [1]. 8 mg of PB were dispersed in 0.3 wt% PSS aqueous solution to absorb the anionic surfactant through sonication for 24 h. After centrifugation, the obtained sample was transferred to a glass vial containing 12 mL of methanol mixed with a certain amount of PVP (0.04−0.08 g), and the mixture was stirred for a short time. Then, 2.0 mL of $Zn(NO_3)_2$ (0.043 M) methanol solution was added into the above mixture, followed by adding 8.0 mL of 2-MeIM (0.043-0.172 M) methanol solution dropwise. After stirring for several hours, the sample was collected by centrifugation and washed with methanol three times. The obtained PB@ZIF-8 sample was dried under vacuum atmosphere for 6 h for future characterization.

1.3. Drug loading and releasing:

The drug loading test was operated by mixing the CSD-MOFs with DOX (2 mg mL^{-1}) in phosphate buffered saline (PBS) (pH=7.4). 2 mg of CSD-MOFs was dispersed into 2 mL water and then added into 1 mL of DOX solution (2 mg/mL) under vortex. The mixture was stirred at room temperature for 24 h under dark conditions, and the DOX-loaded CSD-MOFs were centrifuged for further release tests. The supernatant was collected and measured by UV–vis-NIR spectrophotometer at 480 nm to calculate loading efficiency and content. For release, CSD-MOFs@DOX were packaged into a dialysis bag (MWCO=3500), and then immersed within 10 mL PBS solution at different pH (pH=7.4, 6.2 or 5.0) and temperature (37 or 43 ºC). At different time points, 2.0 mL solution was collected to determine the concentration of DOX, and then 2.0 mL fresh PBS solution was added back. Three independent experiments were carried out to minimize the deviations.

1.4. Measurements of Photothermal Property:

CSD-MOFs aqueous solutions (0, 0.02, 0.05, and 0.2 mg mL^{-1}) were irradiated with an 808 nm laser (1.6 W cm^{-2}) for 10 min. To investigate the photostability of the CSD-MOFs, UV-vis-NIR spectra was measured before and after irradiation. The temperature variation was recorded with a digital thermistor temperature sensor. Besides, thermographs of different solutions were recorded with an infrared thermal camera (ICI7320, Infrared Camera Inc.).

1.5. In Vitro Cellular Toxicity Test:

Human cervical carcinoma (HeLa) cells were cultured in 96-well plates at 10^4 cells

per well and incubated in 5% CO_2 at 37 ºC for 24 h. Then different concentrations of PB and CSD-MOFs (6.75, 13.5, 27, 40.5, 54, and 108 μg mL^{-1}) were added. After that, the cells were further incubated for 24 h, and excess unbound materials were washed for three times with PBS. Subsequently, the relative cell viabilities (%) were detected by the standard MTT assay.

1.6. MRI measurements:

For *in vitro* MRI tests, PB and CSD-MOFs nanocubes at various Fe concentrations (0, 0.125, 0.25, 0.5, 0.75, and 1.5 mM) were measured with a clinical magnetic resonance scanner (GE HDxt, 3.0 T). For *in vivo* MR imaging, we conducted MRI of tumor-bearing female BALB/c nude mice with an average body weight of 18 g (Shanghai SLAC Laboratory animal Co., Ltd.,). Animal experiments were approved by the Animal Care Committee of University of Science and Technology of China and the Ethical Committee of the Experimental Animal Center of Anhui Medical University. Before tail vein injection of CSD-MOFs (2 mg/mL in PBS, 10 mg of per kilogram of mouse body weight), mice were anesthetized through intraperitoneal injection of 10% chloral hydrate. T_1- and T_2*-weighted MR imaging were acquired pre-injection, 30 min, and 24 h post-injection.

1.7. In Vitro Antitumor Activity:

HeLa cells were seeded into 96-well plates and incubated in 5% CO_2 at 37 ºC for 16 h. Then the culture medium was replaced with fresh complete medium containing with PBS (control), free DOX (5.75, 11.5, 23, 34.5, 46, and 92 μg mL^{-1}), CSD-MOFs (6.75, 13.5, 27, 40.5, 54, and 108 μg mL^{-1}), CSD-MOFs@DOX (12.5, 25, 50, 75, 100, and

200 μg mL^{-1}), CSD-MOFs+NIR and CSD-MOFs@DOX+NIR. After incubation for 4 h, excess unbound materials were removed by rinsing three times with PBS. Fresh complete medium was then added to the wells. The cells of CSD-MOFs+NIR and CSD-MOFs@DOX+NIR groups were exposed to an 808 nm laser (1.6 W cm^{-2}, 5 min). Then the cells were further incubated for 24 h, and excess unbound materials were washed for three times with PBS, before standard MTT assay.

1.8. CLSM and Two-photon Fluorescence Analysis:

HeLa cells were seeded on Chambered cover glass (Lab-Tek Chambered 1.0 Borosilicate Cover Glass system, Nunc). After 24 h, the cells were cultured to 50-60% confluency, then incubated with CSD-MOFs nanocubes at 37 ºC in 10% CO_2 atmosphere for 24 h. For subcellular localization, the cells were transfected with mCherry-LAMP-1 (lysosome-associated membrane protein 1), which specifically localized at the lysosome membrane. 24 h after the transfection, CSD-MOFs were added into the medium with incubation for another 24 h. Then the cells were washed with PBS, fixed with 3.7% paraformaldehyde and permeabilized, stained with 4′,6-diamidino-2-phenylindole (DAPI), and imaged by a confocal fluorescence microscope (Zeiss LSM 710).

1.9. Mouse tumor model:

Once palpable tumors in BALB/c nude mice were established for xenograft experiments, they were randomly allocated into six groups (control, NIR, free DOX, CSD-MOFs@DOX, CSD-MOFs+NIR, CSD-MOFs@DOX+NIR, n=5). Free DOX, CSD-MOFs, CSD-MOFs@DOX in PBS buffer (total dose=100 μL,

$C_{[CSD\text{-}MOFs@DOX]}$=1.7 mg mL^{-1}, $C_{[DOX]}$=0.85 mg mL^{-1}, $C_{[CSD\text{-}MOFs}$=1.0 mg mL^{-1}) were injected via the tail vein, while mice in the control group were only injected with PBS (100 μL). After 24 h, the tumors from group 2, 5 and 6 were irradiated with an 808 nm laser (1.6 W cm^{-2}, 5 min). Tumor dimensions were measured with a caliper every 2 days after drug administration, and the tumor volume was calculated according to the equation: Volume=(Tumor length)×(Tumor width)^2/2. The combination index (CI) was calculated by CI=AB/(A×B).[2] AB was the ratio of the combination group to the control group. A or B was the ratio of the single treatment group (chemo- or thermal-therapy) to the control group.

1.10. Blood circulation:

To determine the blood circulation of CSD-MOFs, nanoparticles were injected into the tail vein at dose of 5 mg/kg (n=3). At the predetermined time points, 5 μL blood was extracted and then digested with 0.2 mL aqua regia (HCl/HNO_3=3:1) before analyses of Fe contents using ICP-AES. After subtracting natural Fe in blood determined by measuring the blood sample collected from an untreated mouse, the blood concentrations of Fe were then calculated and presented by unit of the percentage of injected dose per gram tissue (%ID/g).[3]

1.11. Biodistribution of CSD-MOFs *in vivo*:

To study the biodistribution of CSD-MOFs in vivo, the CSD-MOFs solution (10 mg/kg) in PBS was injected into BALB/c mice from the tail vein. After 24 h post administration, mice were sacrificed and organs were dissected and weighed. For ICP-MS assay, each sample was placed in small quartz boat and then the boat was

placed into a tube furnace and heated to 700 ºC in the air and maintained for 4 h so that the organ can be totally burned to ashes. After that the ashes were dissolved in aqua regia to transform oxide to Fe ions. The amount of Fe elements was finally normalized to the tissue weight per gram.

1.12. Pathological Investigation:

The tumor tissues and main organs of the administrated mice were resected, fixed in 4% formalin and then embedded in paraffin blocks. Formalin-fixed paraffin-embedded tissue samples were sectioned, stained with hematoxylin and eosin (H&E) and then examined with microscope. For Ki-67 staining, tumor and organs sections were incubated with the anti-Ki-67 rabbit polyclonal antibody (Abcam, ab15580, America) overnight at 4 ºC. Then, Olympus IX-70 microscope was used to acquire images of the stained tumor and organ slices.

1.13. Characterization:

Transmission electron microscopy (TEM) images were obtained from a transmission electron microscope (Hitachi H-7650) with an accelerating voltage of 100 kV. Powder X-ray diffraction (PXRD) patterns were performed on a Japan Rigaku D/MAX-cAX-ray diffractometer equipped with Cu Ka radiation. High-angle annular dark field (HAADF)-STEM and energy-dispersive X-ray (EDX) analyses were performed on a JEOL ARM-200F field-emission transmission electron microscope operating at 200 kV accelerating voltage. Scanning electron microscopy (SEM) images were acquired on a JEOL JSM-6700M microscopy. The content of Zn and Fe were measured by inductively coupled plasma-atomic emission spectrometer

(ICP-AES) (Optima 7300DV). Ultraviolet-visible (UV-Vis) absorption spectra were measured on a SOLID3700 spectrometer. The dynamic laser light scattering (DLS) measurements were performed with a Zetasizer UV spectrometer (Malvern μV).

2. Supporting figures

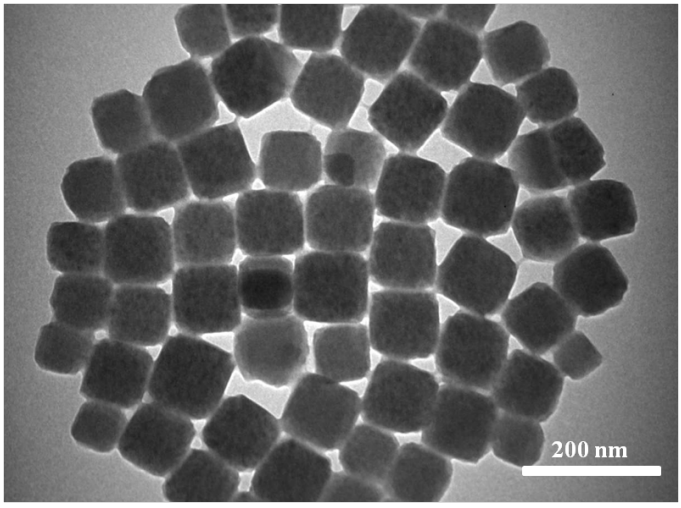

Figure S1. TEM images of PB nanocubes.

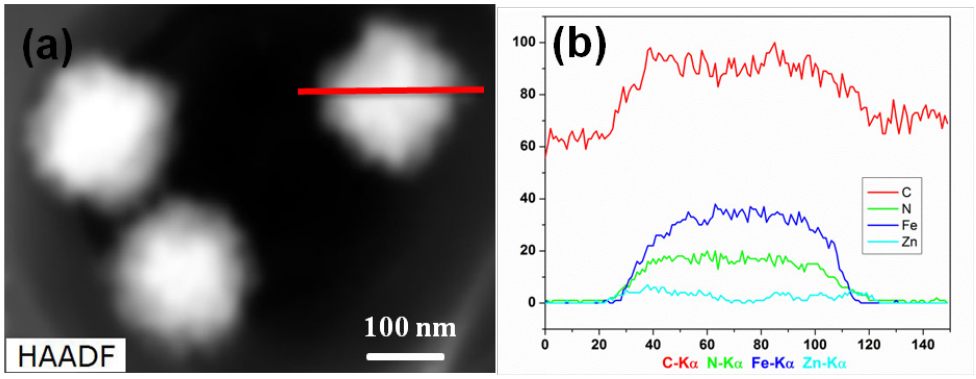

Figure S2. HAADF-STEM image and element line scanning of CSD-MOFs.

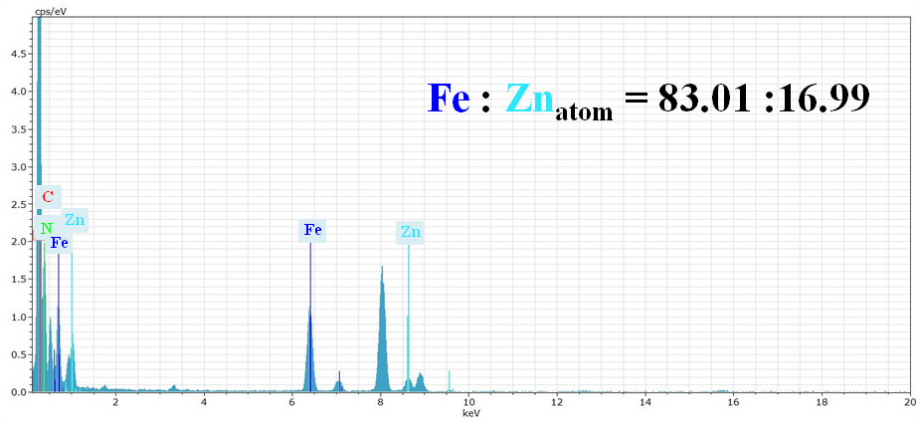

Figure S3. The corresponding EDX spectrum of CSD-MOFs.

Thermogravimetric analysis (TGA): (Figure S4)

Typically, to confirm the weight ratio of PB/ZIF-8, TGA of PB and CSD-MOFs were preformed: Approximately 3-8 mg of samples was used for TGA measurements. Samples were analyzed under an air flow (75 $mL \cdot min^{-1}$) using a Shimadzu-50 thermoanalyser running from 20 ºC to 700 ºC at a heating rate of 10 ºC /min. Herein, it is assumed that water molecules within the materials were evaporated totally when the temperature reaching 180 ºC.

Experimental weight losses of ZIF-8, PB and CSD-MOFs:

(based on TGA datas, Figure S4)

wt % / Item	H_2O	Gas	remnant	Gas /(Gas+remnant)	remnant /(Gas+remnant)
ZIF-8	0	62.28	37.72	62.28	37.72
PB	15.90	40.22	43.88	47.82	52.18
CSD-MOFs	9.14	47.34	43.52	52.1	47.9

Assuming that the weight of ZIF-8 is x g and PB is y g (CSD-MOFs: x + y = 100 g).

62.28% x + 47.82% y = 52.1 g……①

37.72% x + 52.18% y = 47.9 g……..②

So the value of x is 29.6 g and y is 70.4 g.

That is to say the **weight ratio** of ZIF-8/PB is **29.6/70.4**.

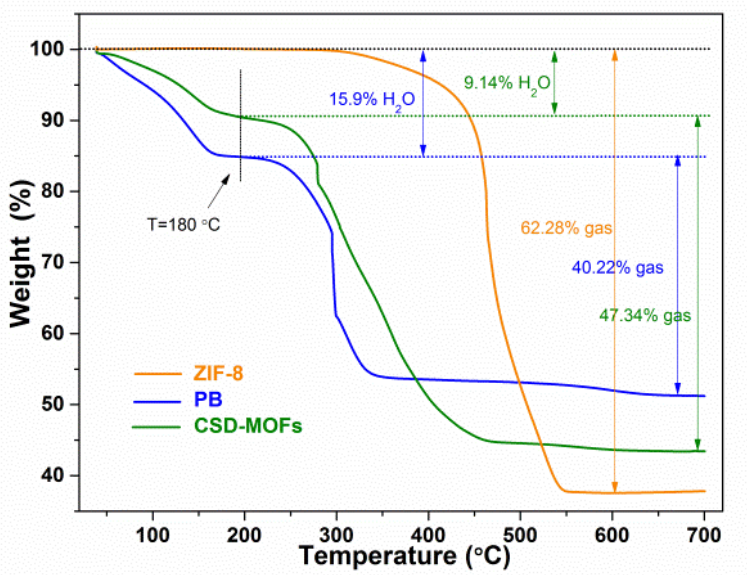

Figure S4. TGA of inner pure ZIF-8, pure PB and CSD-MOFs.

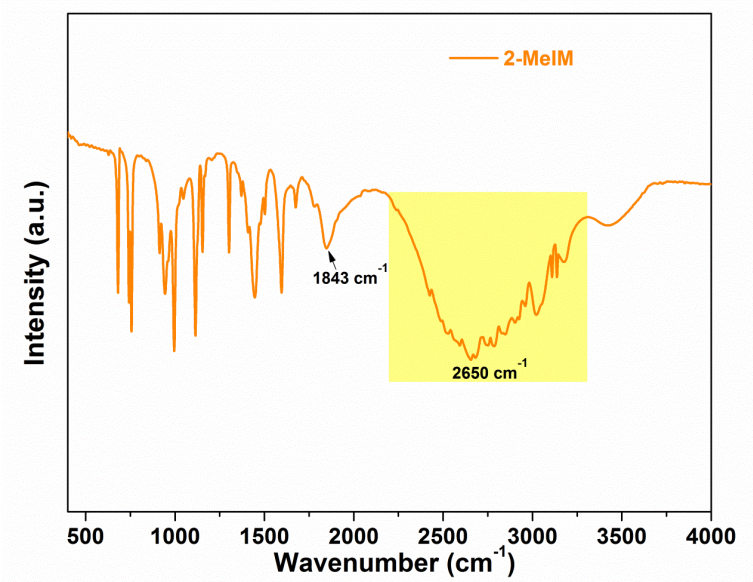

Figure S5. FT-IR spectrum of pure 2-MeIM.

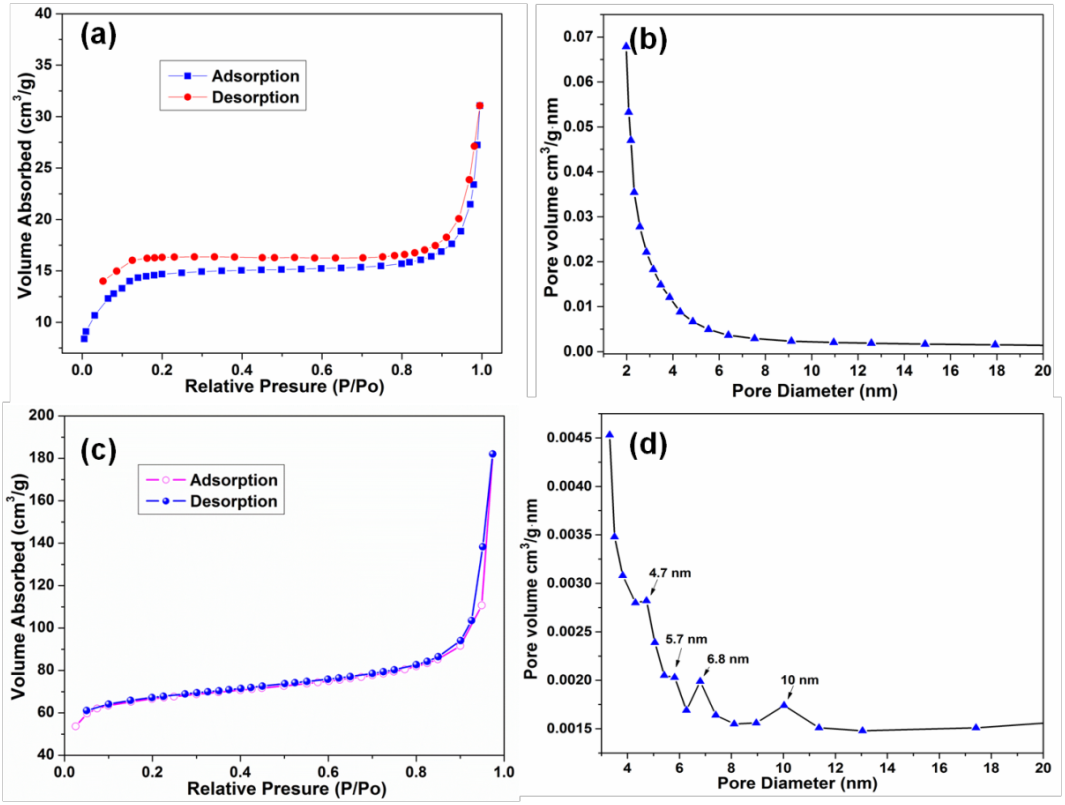

Figure S6. N_2 adsorption-desorption isotherms and corresponding pore size distributions of PB (a) and (b), CSD-MOFs (c) and (d).

Thermogravimetric analysis (TGA): (Figure S7)

TGA of pure DOX and CSD-MOFs@DOX were also preformed to confirm the drug loading capacity of CSD-MOFs. (Figure S7)

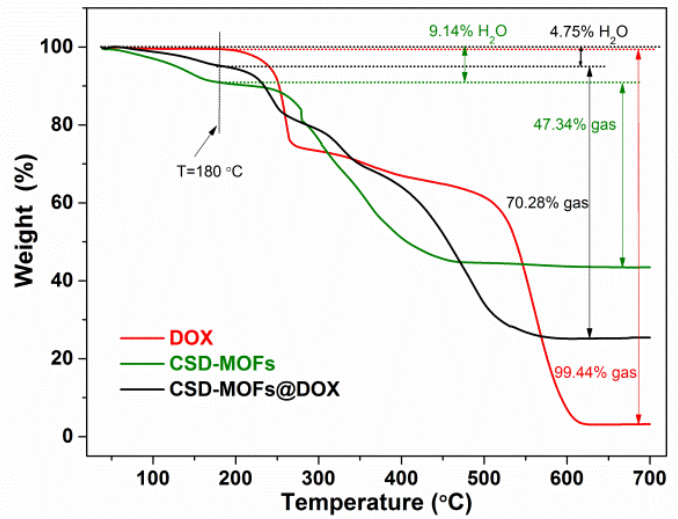

Figure S7. TGA of pure DOX, CSD-MOFs and CSD-MOFs@DOX.

wt % / Item	H_2O	Gas	remnant	Gas /(Gas+remnant)	remnant /(Gas+remnant)
DOX	0.56	99.44	0	100	0
CSD-MOFs	9.14	47.34	43.52	52.1	47.9
CSD-MOFs@DOX	4.75	70.28	24.97	73.8	26.2

Assuming that the weight of DOX is x g and CSD-MOFs is y g (CSD-MOFs@DOX is x+y=100 g).

100%x+52.1%y=73.8 g……①

47.9%y=26.2 g……..②

So the value of x is 45.3 g and y is 54.7 g.

The **loading capacity** is estimated to be **828.15 mg/g** (mg of DOX per g of dry CSD-MOFs) which is slightly lower than UV-vis data.

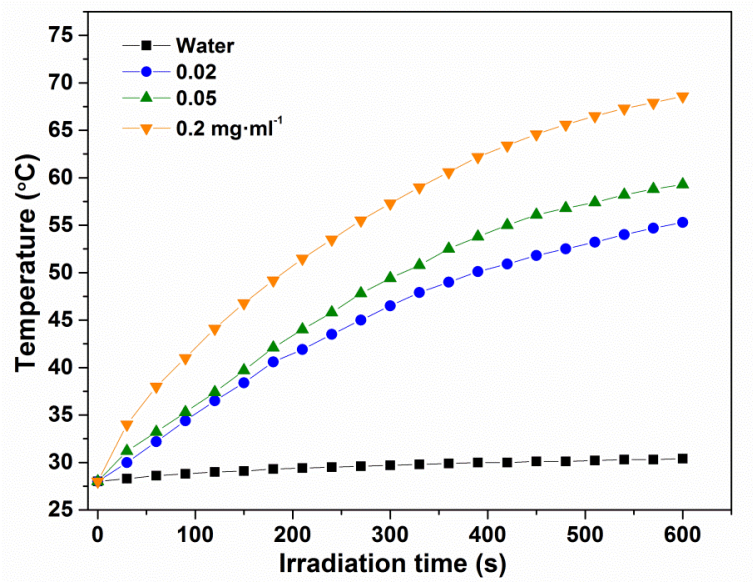

Figure S8. Heating curves of PB solutions of different mass concentrations (0, 0.02, 0.05, 0.2 mg mL^{-1}) under 808 nm laser irradiation at the power density of 1.6 W cm^{-2}.

Calculation of photothermal conversion efficiency: (Figure S9)

The photothermal conversion efficiency of PB and CSD-MOFs were calculated using the model described in Roper's et al.[4] where the photothermal conversion efficiency is described by the following equations:

$$\sum_i m_i C_{p,i} \frac{dT}{dt} = Q_{NPs} + Q_{diss} - Q_{loss} \quad \text{----------(1)}$$

where m and C_p are the mass and heat capacity of solvent (water), respectively. T is the solution temperature. Q_{NPs} is the photothermal energy input by PB or CSD-MOFs.

Q_{diss} is the heat associated with the light absorbance of the solvent. Q_{loss} is thermal energy lost to the surroundings.

$$Q_{NPs} = I(1 - 10^{-A_{808}})\eta \text{ ----------(2)}$$

where η represents the photothermal conversion efficiency. A_{808} is the absorbance intensity of PB or CSD-MOFs at 808 nm. I is the power density of laser (1.6 W/cm^2).

$$Q_{loss} = hS\Delta T \text{ ----------(3)}$$

where h is the heat transfer coefficient. S is the surface area of the container. ΔT is the temperature change of the solution from that of the surroundings.

When the temperature of system reaching a steady stage, dT/dt in equation (1) is 0. Then, $Q_{NPs} + Q_{diss} = Q_{loss} = hS\Delta T_{max}$, and we get equation (4).

$$\eta = \frac{hS\Delta T_{max} - Q_{diss}}{I(1-10^{-A_{808}})} \text{ ----------(4)}$$

To calculate hS: We herein introduce $\theta = \Delta T/\Delta T_{max}$, which is defined as the ratio of ΔT to ΔT_{max}. Then equation (1) will be change to equation (5).

$$\frac{d\theta}{dt} = \frac{hA}{\sum_i m_i C_{p,i}}\left[\frac{Q_{NPs}+Q_{diss}}{hS\Delta T_{max}} - \theta\right] \text{ ----------(5)}$$

When the laser was shut off (the cooling stage), the $Q_{NPs}+Q_{diss} = 0$, equation (5) will be changed to equation (6).

$$t = -\frac{\sum_i m_i C_{p,i}}{hS} \ln\theta \text{ ----------(6)}$$

hA can be determined by plotting time as a function of $-\ln\theta$ for the cooling curves (after switching off the laser) and inputting appriate values for m (1 g) and C_p (4.2 J/g/^{o}C).

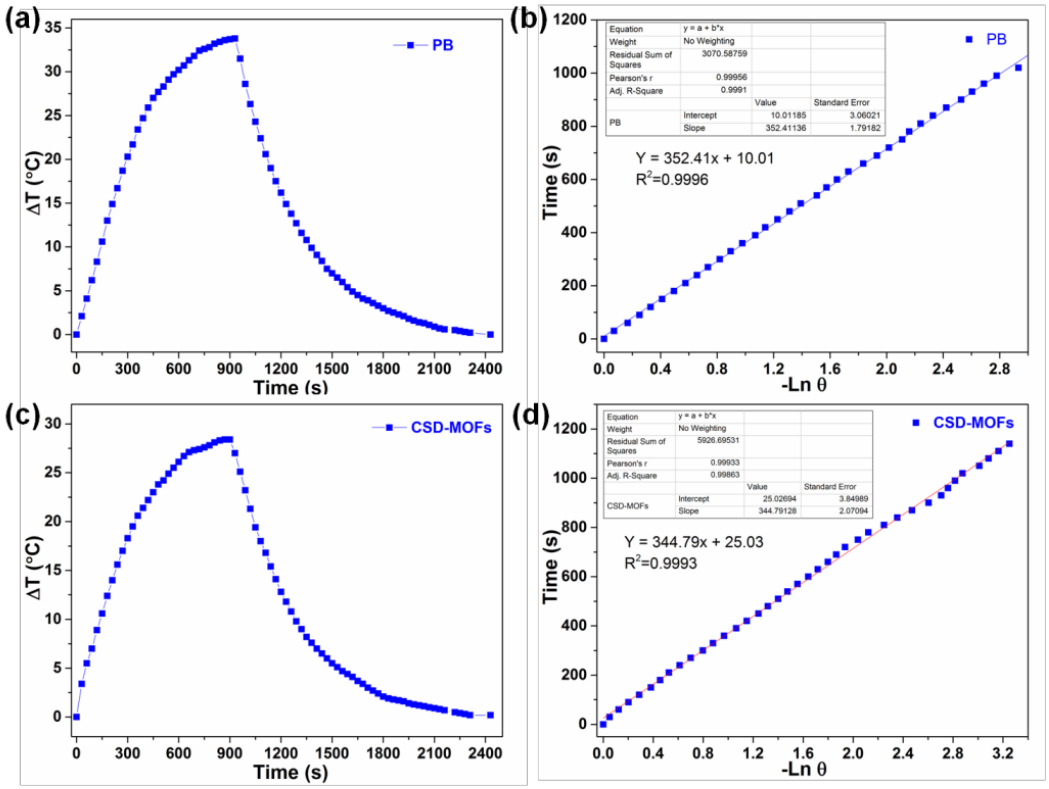

Figure S9. (a) and (c) The photothermal response of PB and CSD-MOFs in water (50 μg mL^{-1}) with laser irradiation (808 nm, 1.6 W cm^{-2}, 5 min) and then the laser was shut off. (b) and (d) Linear time data versus –Lnθ obtained from the cooling period.

Q_{diss} is measured independently to be 0.0389 J/s.

For PB: Where ΔT_{max} is 32.8 ºC, Q_{diss} is measured independently to be 0.0389 J/s, I is 1.6 W/cm^2 and A_{808} is 1.402. According to the linear time data versus –lnθ in Figure S, and inputting appriate values for m (1 g) and C_p (4.2 J/g/ºC) the photothermal conversion efficiency of PB was calculated to be ~22.9 %.

For CSD-MOFs: Where ΔT_{max} is 28.4 ºC, Q_{diss} is measured independently to be 0.0389 J/s, I is 1.6 W/cm^2 and A_{808} is 0.794. According to the linear time data versus –lnθ in Figure S, and inputting appriate values for m (1 g) and C_p (4.2 J/g/ºC) the photothermal conversion efficiency of CSD-MOFs was calculated to be ~22.86 %.

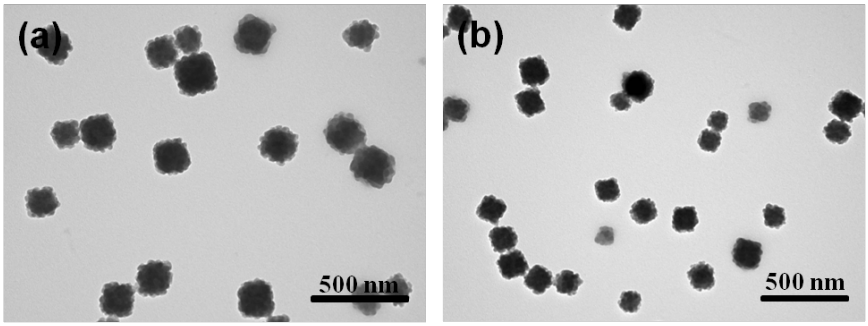

Figure S10. TEM images of CSD-MOFs before (a) and after (b) 808 nm NIR irradiation for 10 min.

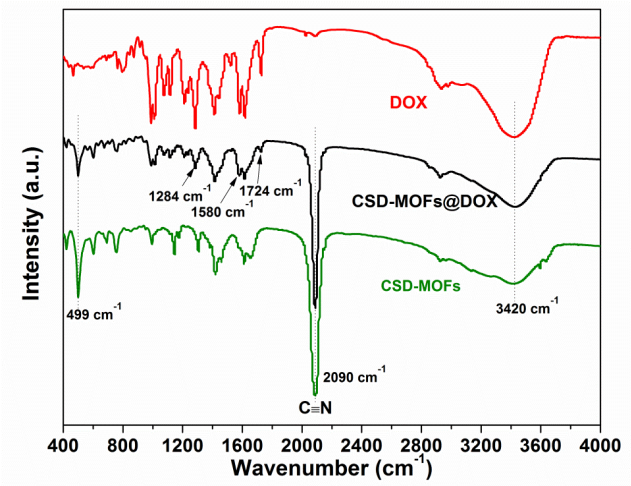

Figure S11. FT-IR spectrum of pure DOX, CSD-MOFs and DOX loaded CSD-MOFs (CSD-MOFs@DOX).

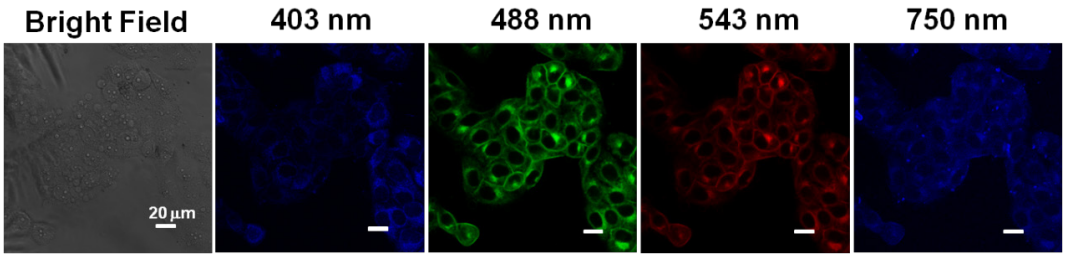

Figure S12. Confocal fluorescence images of HeLa cells incubated with CSD-MOFs@DOX (blue and green fluorescence of CSD-MOFs, red fluorescence of DOX).

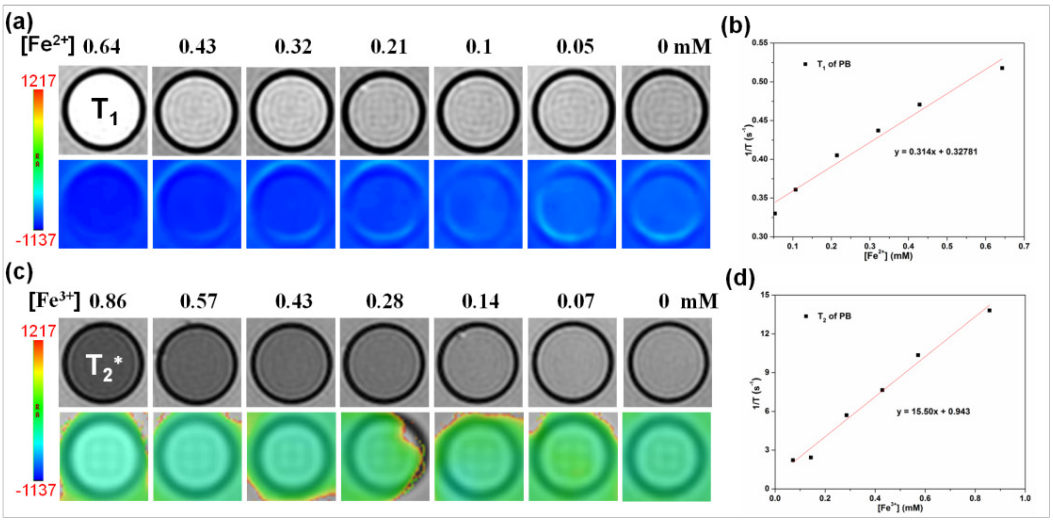

Figure S13. *In vitro* MRI test: (a) T_1 and (b) T_2^* weighted MR images of PB with different concentrations of Fe. (c) T_1 and (d) T_2^* relaxation rates as a function of Fe concentration of PB.

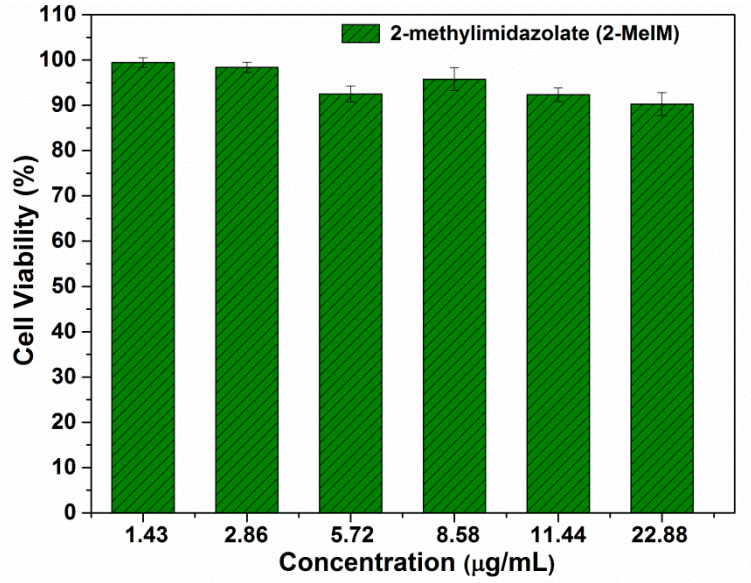

Figure 14. *In vitro* cytotoxicity of 2-MeIM (the same concentration of 2-MeIM in CSD-MOFs).

Hemolysis assay: (Figure S15)

Hemolysis assay of CSD-MOFs was performed. Typically, 1 mL of fresh mouse blood (heparin sodium stabilized) was centrifuged and washed with PBS for several times to obtain red blood cells (RBCs). Then, 0.3 mL of diluted RBCs suspension (volume ratio of red blood cells and PBS is 1:10) was mixed with 1.2 mL of deionized water, 1.2 mL of PBS, and 1.2 mL of CSD-MOFs suspensions with various concentrations of 16, 32, 63, 125, 250, 500, and 1000 μg/mL, respectively. After the nine tubes were shaken in a rotating manner and allowed to rest for 3 h, the absorbance of the upper supernatants was detected by UV–vis spectroscopy at 540 nm.

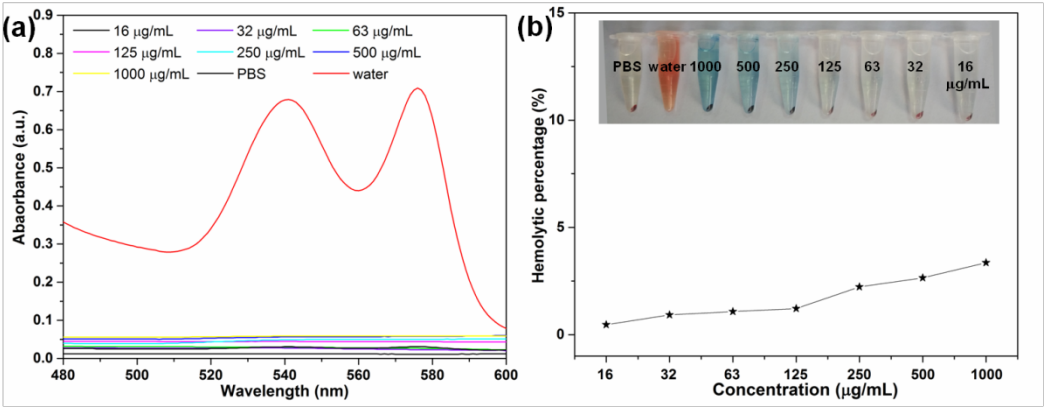

Figure S15. Hemolytic activity of CSD-MOFs at different concentrations. (a) UV−vis spectrum of supernatant solutions of RBCs incubated with different concentrations of CSD-MOFs. (B) Hemolytic percentages of RBCs treated with different concentrations of CSD-MOFs solution for 3 h. The inset images are for direct observation of the results, suggesting the good biocompatibility of CSD-MOFs.

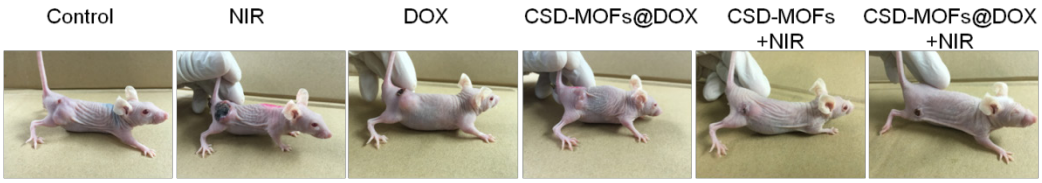

Figure S16. Images of a representative mouse from each group captured on 19th day after the treatment.

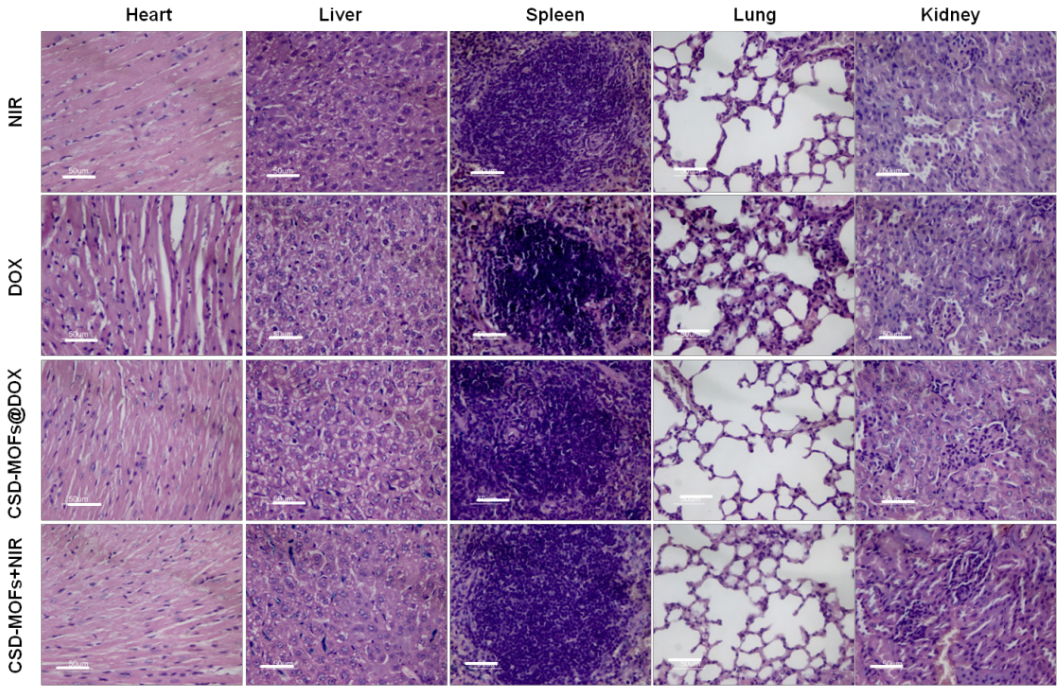

Figure S17. H&E stained images of major organs of mice from differently treated groups at 19th day. (All the scale bar: 50 μm).

Blood Smear: (Figure S18)

To assess the toxicity of CSD-MOFs to blood cells, mouse blood was mixed with CSD-MOFs. In a typical experiment, CSD-MOFs were incubated with fresh mouse whole blood for 4 h at a final concentration of 100 μg/mL. Same amount of PBS incubated with whole blood was used as negative control. A drop of incubated blood was put on a slide and spread using another slide. After the smears were dried, samples were fixed with methyl alcohol, then stained diluted Giemsa stain. Slides were then washed with water, air dried and observed under a microscope.

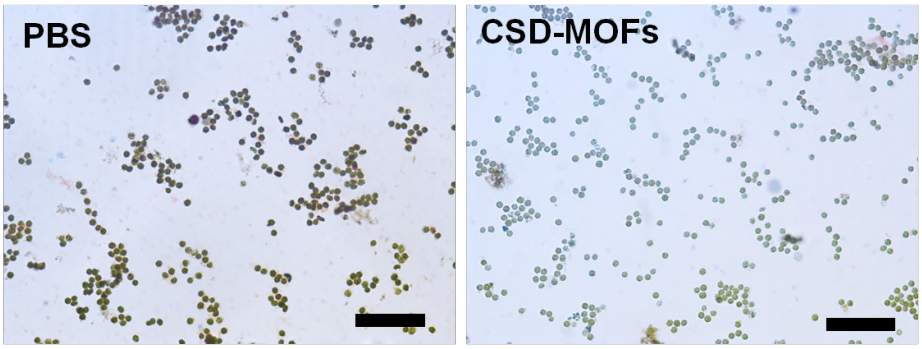

Figure S18. Blood smear test of CSD-MOFs treated blood cells. Scale bar = 50 μm.

Reference:

1. Wang D, Zhou J, Chen R, Shi R, Zhao G, Xia G, et al. Controllable synthesis of dual-MOFs nanostructures for pH-responsive artemisinin delivery, magnetic resonance and optical dual-model imaging-guided chemo/photothermal combinational cancer therapy. Biomaterials. 2016; 100: 27-40.

2. Tian L, Chen Q, Yi X, Wang G, Chen J, Ning P, et al. Radionuclide I-131 Labeled Albumin-Paclitaxel Nanoparticles for Synergistic Combined Chemo-radioisotope Therapy of Cancer. Theranostics. 2017; 7: 614-23.

3. Li Z, Wang C, Cheng L, Gong H, Yin S, Gong Q, et al. PEG-functionalized iron oxide nanoclusters loaded with chlorin e6 for targeted, NIR light induced, photodynamic therapy. Biomaterials. 2013; 34: 9160-70.

4. Roper DK, Ahn W, Hoepfner M. Microscale Heat Transfer Transduced by Surface Plasmon Resonant Gold Nanoparticles. The journal of physical chemistry C, Nanomaterials and interfaces. 2007; 111: 3636-41.